JACS
JOURNAL OF THE AMERICAN CHEMICAL SOCIETY

Subscriber access provided by American Chemical Society

Article

Molecular Rotor of Cs([18]crown-6) in the Solid State Coupled with the Magnetism of [Ni(dmit)]

Tomoyuki Akutagawa, Kozo Shitagami, Sadafumi Nishihara, Sadamu Takeda, Tatsuo Hasegawa, Takayoshi Nakamura, Yuko Hosokoshi, Katsuya Inoue, Satoshi Ikeuchi, Yuji Miyazaki, and Kazuya Saito

J. Am. Chem. Soc., **2005**, 127 (12), 4397-4402• DOI: 10.1021/ja043527a • Publication Date (Web): 26 February 2005

Downloaded from http://pubs.acs.org on March 24, 2009

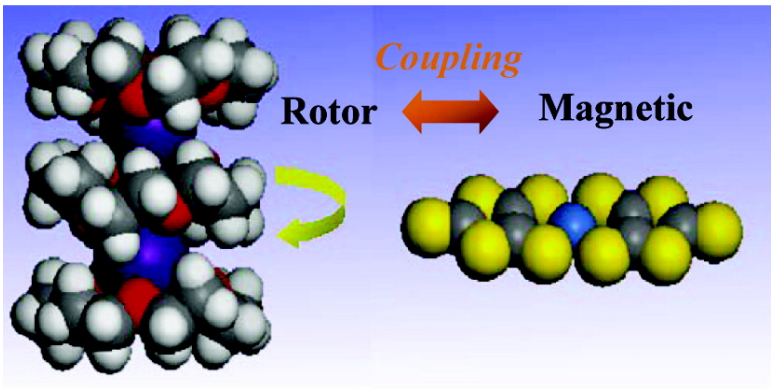

More About This Article

Additional resources and features associated with this article are available within the HTML version:

- Supporting Information
- Links to the 10 articles that cite this article, as of the time of this article download
- Access to high resolution figures
- Links to articles and content related to this article
- Copyright permission to reproduce figures and/or text from this article

View the Full Text HTML

ACS Publications
High quality. High impact.

Journal of the American Chemical Society is published by the American Chemical Society. 1155 Sixteenth Street N.W., Washington, DC 20036

J|A|C|S
ARTICLES
Published on Web 02/26/2005

Molecular Rotor of $Cs_2([18]crown\text{-}6)_3$ in the Solid State Coupled with the Magnetism of $[Ni(dmit)_2]$

Tomoyuki Akutagawa,*[,†,‡,¶] Kozo Shitagami,[‡] Sadafumi Nishihara,[‡] Sadamu Takeda,[⊥] Tatsuo Hasegawa,[†,‡] Takayoshi Nakamura,*[,†,‡,¶] Yuko Hosokoshi,[||] Katsuya Inoue,[||] Satoshi Ikeuchi,[§] Yuji Miyazaki,[§] and Kazuya Saito[§]

Contribution from the Research Institute for Electronic Science, Hokkaido University, Sapporo 060-0812, Japan, Graduate School of Environmental Earth Science, Hokkaido University, Sapporo 060-0810, Japan, CREST, Japan Science and Technology Corporation (JST), Kawaguchi 332-0012, Japan, Graduate School of Science, Hokkaido University, Sapporo 060-0810, Japan, Institute for Molecular Science, Okazaki 444-8585, Japan, and Research Center for Molecular Thermodynamics, Graduate School of Science, Osaka University, Toyonaka, Osaka 560-0043, Japan

Received October 26, 2004; E-mail: takuta@imd.es.hokudai.ac.jp (T.A.); tnaka@imd.es.hokudai.ac.jp (T.N.)

Abstract: Nanoscale molecular rotors that can be driven in the solid state have been realized in $Cs_2([18]crown\text{-}6)_3[Ni(dmit)_2]_2$ crystals. To provide interactions between the molecular motion of the rotor and the electronic system, $[Ni(dmit)_2]^-$ ions, which bear one $S = {}^1/_2$ spin on each molecule, were introduced into the crystal. Rotation of the [18]crown-6 molecules within a $Cs_2([18]crown\text{-}6)_3$ supramolecule above 220 K was confirmed using X-ray diffraction, NMR, and specific heat measurements. Strong correlations were observed between the magnetic behavior of the $[Ni(dmit)_2]^-$ ions and molecular rotation. Furthermore, braking of the molecular rotation within the crystal was achieved by the application of hydrostatic pressure.

Introduction

Molecular motors serve as important nanoscale molecular machines for energy conversion and in the transport of substances in biological systems.[1,2] Biological molecular machines, such as ATPase in cell membranes, actin/myosin in muscles, and kinesin motor on microtubes, yield significantly high energy conversion efficiencies of up to nearly 100%.[1,3−5] In these biological machines, the energy needed to operate the nanoscale motors is supplied chemically from a nonequilibrium energy gradient under thermal fluctuations within the limits of the second law of thermodynamics.[2]

With energy conversion efficiencies comparable to those of highly efficient biological motors, artificial molecular motors can be utilized for nanoscale electronic devices such as quantum electronic pumps and quantum ratchets.[6,7] Adiabatic unidirectional molecular rotors can be applied to novel energy conversion systems that can extract kinetic energy via Maxwell's demon within the second law of thermodynamics. The successful design of artificial molecular motors as components of molecular machines involves several important points: (i) construction in the solid state, (ii) effective utilization of thermal noise, (iii) injection of external energy, except as chemical energy, to bias the rotation, and (iv) coupling of the molecular rotation with electronic systems. Molecular rotors coupled with electrical and magnetic properties can be developed into novel energy conversion systems based on the kinetic energy of unidirectional molecular rotation in the solid state to electromagnetic energies.

Several attempts to synthesize nanoscale molecular motors have been reported.[8−12] Unidirectional rotary motion in solution was successfully realized using photochemical/thermal isomer-

† Research Institute for Electronic Science, Hokkaido University.
‡ Graduate School of Environmental Earth Science, Hokkaido University.
¶ CREST, JST.
⊥ Graduate School of Science, Hokkaido University.
|| Institute for Molecular Science.
§ Research Center for Molecular Thermodynamics, Graduate School of Science, Osaka University.

(1) Stryer, L. *Biochemistry*; Freeman: New York, 1995.
(2) *Molecular Machines and Motors*; Sauvage, J.-P., Ed.; Springer: Berlin, 2001.
(3) Kitamura, K.; Tokunaga, M.; Iwane, A.; Yanagida, T. *Nature* **1999**, *397*, 129.
(4) Funatsu, T.; Harada, Y.; Tokunaga, M.; Saito, K.; Yanagida, T. *Nature* **1995**, *374*, 555.
(5) Astumian, R. D. *Science* **1997**, *276*, 917.
(6) Switkes, M.; Marcus, C. M.; Campman, K.; Gossard, A. C. *Science* **1999**, *283*, 1905.
(7) Linke, H.; Humphrey, T. E.; Löfgren, A.; Sushkov, A. O.; Newbury, R.; Taylor, R. P.; Omling, P. *Science* **1999**, *286*, 2314.
(8) (a) *Molecular Devices and Machines*; Balzani, V., Venturi, M., Dredi, A., Eds.; Wiley-VCH: Weinheim, 2003. (b) *Molecular Switches*; Feringa, B. L., Ed.; Wiley-VCH: Weinheim, 2001.
(9) Molecular Machines Special Issue. *Acc. Chem. Res.* **2001**, *34*, 412.
(10) (a) Koumura, N.; Zijlstra, R. W. J.; Delden, R. A.; Harada, N.; Feringa, B. L. *Nature* **1999**, *401*, 152. (b) Koumura, N.; Geertsema, E. M.; Meetsma, A.; Feringa, B. L. *J. Am. Chem. Soc.* **2000**, *122*, 12005.
(11) (a) Dominguez, Z.; Dang, H.; Strouse, M. J.; Garcia-Garibay, M. A. *J. Am. Chem. Soc.* **2002**, *124*, 7719. (b) Dominguez, Z.; Dang, H.; Strouse, M. J.; Garcia-Garibay, M. A. *J. Am. Chem. Soc.* **2002**, *124*, 2398. (c) Godinez, C. E.; Zepeda, G.; Garcia-Garibay, M. A. *J. Am. Chem. Soc.* **2002**, *124*, 4701. (d) Dominguez, Z.; Khuong, T. V.; Dang, H.; Sanrame, C. N.; Nuñez, J. E.; Garcia-Garibay, M. A. *J. Am. Chem. Soc.* **2003**, *125*, 8827. (e) Godinez, C. E.; Zepeda, G.; Mortko, C. J.; Dang, H.; Garcia-Garibay, M. A. *J. Org. Chem.* **2004**, *69*, 1652.
(12) Leigh, D. A.; Wong, J. Y.; Dehez, F.; Zerbetto, F. *Nature* **2003**, *424*, 174.

Table 1. Selected Temperature-Dependent Crystal Parameters of Salt **1**

	temperature, K						
	100	145	180	210	180	260	300
a, Å	10.7634(9)	10.7902(7)	10.810(2)	10.804(1)	10.810(2)	10.774(3)	10.787(3)
b, Å	12.8715(9)	12.9099(7)	12.929(3)	12.906(2)	12.929(3)	12.977(5)	13.061(4)
c, Å	13.466(1)	13.4876(8)	13.526(3)	13.573(2)	13.526(3)	13.751(3)	13.808(3)
α, deg	84.967(4)	84.719(3)	84.430(6)	84.226(4)	84.430(6)	84.03(1)	83.94(1)
β, deg	87.007(4)	86.876(3)	86.974(6)	87.300(4)	86.974(6)	88.06(1)	88.09(1)
γ, deg	80.751(3)	80.733(3)	80.520(9)	80.552(3)	80.520(9)	80.62(1)	80.613(9)
V, Å^3	1832.9(2)	1844.9(2)	1854.5(6)	1856.5(4)	1854.5(6)	1886.3(9)	1908.4(8)
D_{calc}, g cm^{-3}	1.777	1.765	1.831	1.754	1.831	1.727	1.832
μ, cm^{-1}	21.23	21.10	21.05	20.96	21.05	20.63	20.47
no. of reflns measd	8140	8182	7906	7907	7906	7890	8008
no. of indep reflns used	7177	7077	6128	5576	6128	5288	4812
$\sigma(I)$	3	3	3	3	3	2.6	2.80
R^a	0.021	0.021	0.039	0.070	0.039	0.052	0.050
$R_w{}^a$	0.026	0.031	0.071	0.077	0.071	0.079	0.048
GOF	1.25	1.18	0.89	0.11	0.89	0.39	0.43

[a] $R = \sum||F_o| - |F_c||/\sum|F_o|$ and $R_w = [\sum(\omega(F_o^2 - F_c^2)^2)/\sum\omega(F_o^2)^2]^{1/2}$.

Scheme 1. Molecular Rotor of Cs_2([18]crown-6)$_3$ and Magnetic System of [Ni(dmit)$_2$], Which Bear One $S = {}^1/_2$ Per Molecule, Coupled within the Crystal

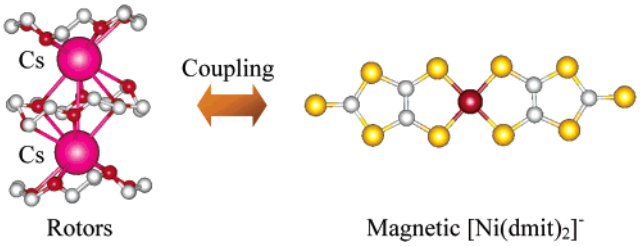

ization and chemical energy.[10,12] The first step in obtaining molecular rotors in the solid state is to introduce loosely packed rotary structures that are connected through weak intermolecular forces, and accordingly, the supramolecular approach should be useful for this purpose. When the thermal energies (k_BT) supplied to the molecular rotors are much greater than that which overcomes the potential barriers of molecular rotation, random rotations with large amplitudes occur, even in the solid state. Biasing mechanisms of the random rotation, as well as asymmetric potential field of the rotational coordinates, cause the unidirectional rotation of the molecular rotors. In these cases, the energy required for biasing the random rotation can be introduced as external stimuli, including physical stimuli such as temperature, pressure, or electromagnetic force, which are preferable to chemical energy within the crystal. These external stimuli can act to perturb the asymmetric potential field, resulting in the unidirectional rotation of thermally fluctuating molecular rotors.

Various types of supramolecular cation structures, based on inorganic cations and crown ethers, have been introduced into [Ni(dmit)$_2$]-based (dmit^{2-} = 2-thioxo-1,3-dithiole-4,5-dithiolate) molecular conductors and magnets.[13−16] One such example involved the molecular conductors $(Li^+)_{0.6}$([15]crown-5)[Ni(dmit)$_2$]$_2$(H$_2$O) and $(Li^+)_{0.8}$([18]crown-6)[Ni(dmit)$_2$]$_2$, which feature the translational motion of lithium ions within the ionic channel structure of a regular stack of crown ethers, influencing the electrical properties of the [Ni(dmit)$_2$] conducting columns.[14,15]

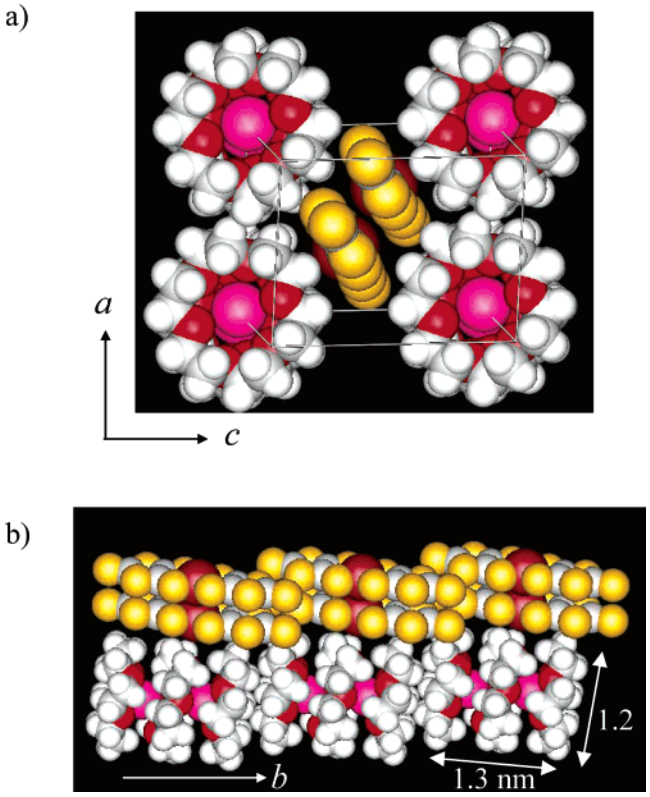

Figure 1. Crystal structure of Cs_2([18]crown-6)$_3$[Ni(dmit)$_2$]$_2$ (T = 100 K). (a) Unit cell viewed along the *b*-axis. [Ni(dmit)$_2$]$^-$ anions formed π-dimers, and Cs_2([18]crown-6)$_3$ stacked along the *b*-axis. (b) π-Dimer chain of [Ni(dmit)$_2$]$^-$ anions and Cs_2([18]crown-6)$_3$ stacking along the *b*-axis.

Our studies involved the introduction of a cylindrical supramolecular cation, Cs_2([18]crown-6)$_3$, into a magnetic [Ni(dmit)$_2$]$^-$ crystal (Scheme 1). Within the crystal, [18]crown-6 showed a molecular rotation, strongly coupled with the magnetic exchange interaction of the [Ni(dmit)$_2$]$^-$ π-dimer

(13) Nakamura, T.; Akutagawa, T.; Honda, K.; Underhill, A. E.; Coomber, A. T.; Friend, R. H. *Nature* **1998**, *394*, 159.
(14) (a) Akutagawa, T.; Nakamura, T.; Inabe, T.; Underhill, A. E. *J. Mater. Chem.* **1996**, *7*, 135. (b) Akutagawa, T.; Nezu, Y.; Hasegawa, T.; Nakamura, T.; Sugiura, K.; Sakata, Y.; Inabe, T.; Underhill, A. E. *Chem. Commun.* **1998**, 2599. (c) Akutagawa, T.; Hasegawa, T.; Nakamura, T.; Takeda, S.; Inabe, T.; Sugiura, K.; Sakata, Y.; Underhill, A. E. *Inorg. Chem.* **2000**, *39*, 2645. (d) Akutagawa, T.; Hasegawa, T.; Nakamura, T.; Takeda, S.; Inabe, T.; Sugiura, K.; Sakata, Y.; Underhill, A. E. *Chem. Eur. J.* **2001**, *7*, 4902.
(15) Akutagawa, T.; Hasegawa, T.; Nakamura, T.; Inabe, T. *J. Am. Chem. Soc.* **2002**, *124*, 8903.
(16) Nishihara, S.; Akutagawa, T.; Hasegawa, T.; Nakamura, T. *Chem. Commun.* **2002**, 408.

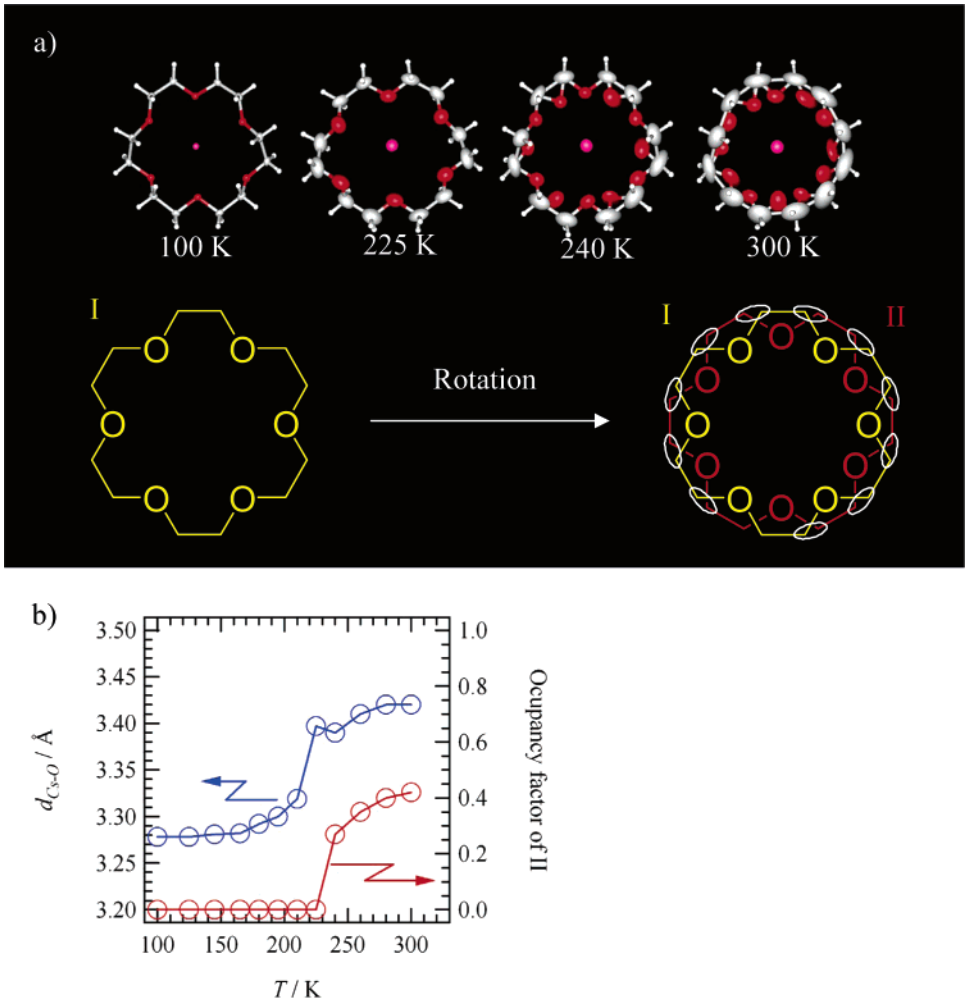

Figure 2. Temperature-induced molecular rotation of $Cs_2([18]crown\text{-}6)_3$ unit in the crystal. (a) Temperature dependence of the crystal structure, showing that [18]crown-6 has two orientations (**I** and **II**) above 240 K. (b) Temperature dependence of the average Cs−O distance (left scale) and occupancy factor of [18]crown-6 of orientation **II** (right scale).

structure, and powerfully influenced the magnetic properties arising from the π-spins ($S = {}^1/_2$) localized on $[Ni(dmit)_2]^-$ anions. Braking of these molecular rotors for the perturbation of the potential energy of rotational coordinates can be achieved by applying pressure as the external stimulus.

Experimental Section

Preparation of [Ni(dmit)$_2$] Salts. The precursor monovalent (n-Bu_4N)[$Ni(dmit)_2$] salt was prepared according to literature.[17] CsI was recrystallized from CH_3CN (distilled prior to use). The crystals were grown using the standard diffusion methods in a vial (~50 mL). The green-colored solution of (n-Bu_4N)[$Ni(dmit)_2$] (20 mg in ~20 mL of CH_3CN) was poured into a CH_3CN solution (~20 mL) of CsI (50 mg) and [18]crown-6 (1 g). Since the density of the former solution was lower than that of the latter one, slow diffusion between the upper and lower liquid layers occurred. After 1 week, single crystals with a typical dimension of 0.5 × 0.5 × 0.4 mm^3 were obtained as black blocks. The stoichiometry of the crystals was determined by X-ray structural analysis and elemental analysis. Anal. Calcd for $C_{24}H_{36}O_9S_{10}NiCs$: C, 29.39; H, 3.70; N, 0.00. Found: C, 29.30; H, 3.61; N, 0.00.

Crystal Structure Determination. Crystallographic data (Table 1) were collected by a Rigaku Raxis-Rapid diffractometer using Mo Kα ($\lambda = 0.71073$ Å) radiation from a graphite monochromator. Structure refinements were performed using the full-matrix least-squares method on F^2. Calculations were performed using the Crystal Structure software package.[18] Parameters were refined using anisotropic temperature factors, except for hydrogen atoms.

Magnetic Susceptibility. The magnetic susceptibility was measured using a Quantum Design model MPMS-5 SQUID magnetometer for polycrystalline samples. The applied magnetic field was 1 T for all measurements. Hydrostatic pressure was applied by using a Be−Ti clamp cell and pressure media (FOMBLINR oil, Ausimont div., YH-VAC140/13). The pressure was corrected by using the transition temperature of Pb from the metallic to a superconducting state.[19]

Calculation of Transfer Integrals. The transfer integrals (t) were calculated within the tight-binding approximation using the extended Hückel molecular orbital method. The LUMO of the [$Ni(dmit)_2$] molecule was used as the basis function.[20] Semiempirical parameters for Slater-type atomic orbitals were obtained from the literature.[20] The t values between each pair of molecules were assumed to be proportional to the overlap integral (S) via the equation $t = -10S$ eV.

Solid-State NMR. The solid-state wide-line ^{1}H NMR spectrum of the sample under static conditions was measured by solid echo pulse

(17) Steimecke, G.; Sieler, H. J.; Krimse, R.; Hoyer, E. *Phosphorus Sulfur* **1979**, *7*, 49.
(18) *Crystal Structure: Single-crystal structure analysis software*, Ver. 3.6; Rigaku Corporation and Molecular Structure Corporation, 2004.
(19) Hosokoshi, Y.; Mito, M.; Tamura, M.; Takeda, K.; Inoue, K.; Kinoshita, M. *Rev. High-Pressure Sci. Technol.* **1988**, *7*, 620.
(20) Mori, T.; Kobayashi, A.; Sasaki, Y.; Kobayashi, H.; Saito, G.; Inokuchi, H. *Bull. Chem. Soc. Jpn.* **1984**, *57*, 627.

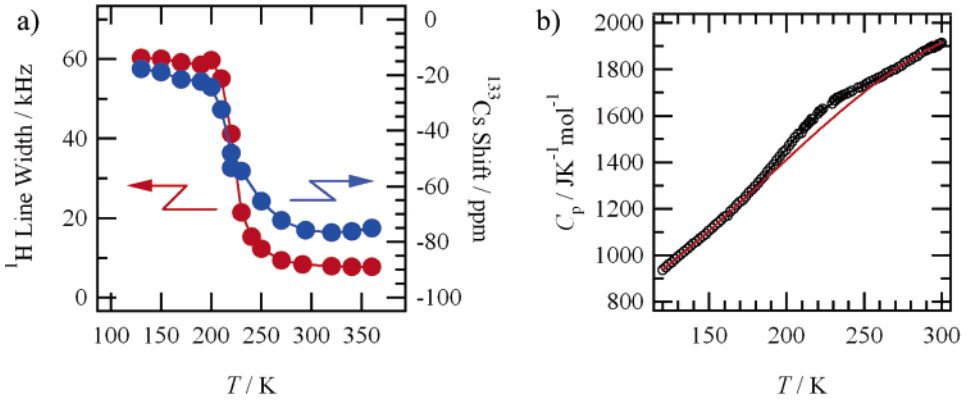

Figure 3. Solid-state NMR and specific heat. (a) Temperature dependence of the line width of the ^{1}H NMR (red) spectra and the chemical shifts of Cs in the ^{133}Cs NMR (blue) of a polycrystalline sample of salt **1**. The chemical shifts represent the maximum position of the spectrum and are not the isotropic shifts. The shifts of the Cs signal were determined using a 4 M CsCl aqueous solution as an external reference. (b) Temperature dependence of the specific heat (C_p). The background is represented as a red line.

sequence $\pi/2_x-\tau-\pi/2_y$ (the $\pi/2$ pulse width and τ were 1.0 and 10 μs, respectively), using a Bruker DSX 300 spectrometer at an operating frequency of 300 MHz for protons. The solid-state wide-line ^{133}Cs NMR spectrum of the sample under static conditions was measured using single pulse of 2.0 μs width at a resonance frequency of 39.4 MHz. The line shape of the spectrum showed a characteristic feature of chemical shift anisotropy. The magic angle spinning NMR spectrum was also measured at room temperature. The full-width at half-maximum was 50 Hz at the spinning speed of 7 kHz. Fine structure of second-order quadrupole coupling was not detected.

Heat Capacity. Heat capacity measurement on salt **1** was performed by a heat-pulse method using a laboratory-made adiabatic calorimeter. Polycrystalline salt **1** (ca. 1 g) was sealed in a gold-plated copper sample vessel (ca. 3 cm^3 in volume) with atmospheric helium gas as the heat exchange medium.

Results and Discussion

As shown in Figure 1, the crystal structure of salt **1** features a supramolecular cation of Cs_2([18]crown-6)$_3$ that possess a club-sandwich structure with a diameter of 1.2 nm and a height of 1.3 nm. The cation stack generated a pseudo-channel structure along the *b*-axis. The [Ni(dmit)$_2$]$^-$ anions (bearing one $S = {}^1/_2$ spin for each [Ni(dmit)$_2$]$^-$ ion) formed a π-dimer structure, which was surrounded by four supramolecular cations. The π-plane of the [Ni(dmit)$_2$]$^-$ dimer was in contact with the cylindrical Cs_2([18]crown-6)$_3$ unit.

Temperature-dependent X-ray structural analyses of salt **1** revealed the rotational motion of the [18]crown-6 within the crystal (Figure 2a). Only the fixed orientation **I** was observed for [18]crown-6 at 100 K, whereas a disordered structure was observed at 300 K in which two [18]crown-6 molecules overlap (orientations **I** and **II**) at a 30° rotational angle to each other. Because one of the [18]crown-6 orientations (orientation **II**) was detected above 240 K, the disorder of [18]crown-6 observed using X-ray analysis was attributed to the thermally induced rotation of the cation structures. In fact, the occupancy factor of orientation **II** showed a thermally activated behavior; the occupancy factor at 240 K was 0.27, which increased to 0.50 (saturation) at 300 K (Figure 2b).

The solid-state wide-line ^{1}H NMR spectra of salt **1** clearly indicated the rotation of [18]crown-6 in the crystal (Figure 3a). The line width was dependent on the temperature, indicating motional narrowing above 250 K (~10 kHz). Furthermore, at ~220 K, the line widths abruptly increased with decreasing

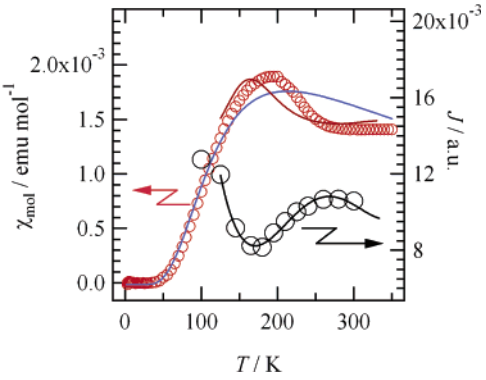

Figure 4. Temperature-dependent magnetic susceptibility (χ_{mol}) per one [Ni(dmit)$_2$]$^-$ molecule (left scale) and the intradimer magnetic exchange energy (J) estimated from the intradimer transfer integral (t_1) (right scale) of salt **1**. The fit using the S−T model calculated from the $\chi_{mol}-T$ behavior below 200 K is indicated as a blue curve. Temperature-dependent J values were applied to fit the $\chi_{mol}-T$ behavior above 150 K (brown curve, see text).

temperatures. Below 200 K, the line width was nearly constant at ~60 kHz. On the basis of the change in the line width at ~220 K, the rotary speed of [18]crown-6 was estimated as several tenths of a kilohertz. The temperature-dependent spectral changes followed the thermally activated behavior of the rotation of [18]crown-6 in the solid phase, which is consistent with the results of X-ray structural analysis. A sudden change in the chemical shifts in the ^{133}Cs NMR spectra was also evident at ~220 K. The chemical shifts of Cs ions are influenced by the motion of [18]crown-6 through interactions between the Cs ions and the oxygen atoms. As shown by X-ray diffraction (Figure 2b), the longer distances of the Cs−O (3.41 Å) above 220 K than that (3.28 Å) below 220 K, associated with the molecular rotation, corresponded to the decreased interactions between the Cs ions and the oxygen atoms of [18]crown-6, causing an upfield shift of the NMR signals.

To evaluate molecular rotation thermodynamically, the specific heat (C_p) of the crystals was measured. The temperature dependence of the specific heat (C_p) is shown in Figure 3b (background is indicated as a red line, C_b). The maximum of C_{ex} ($C_p - C_b$) was observed at ~220 K, which is in good agreement with the results of the NMR and X-ray measurements. The entropy of the transition calculated from C_{ex} was 52 J K^{-1} mol^{-1}, which is equal to $3R \ln 2^3$ (where R is the gas constant),

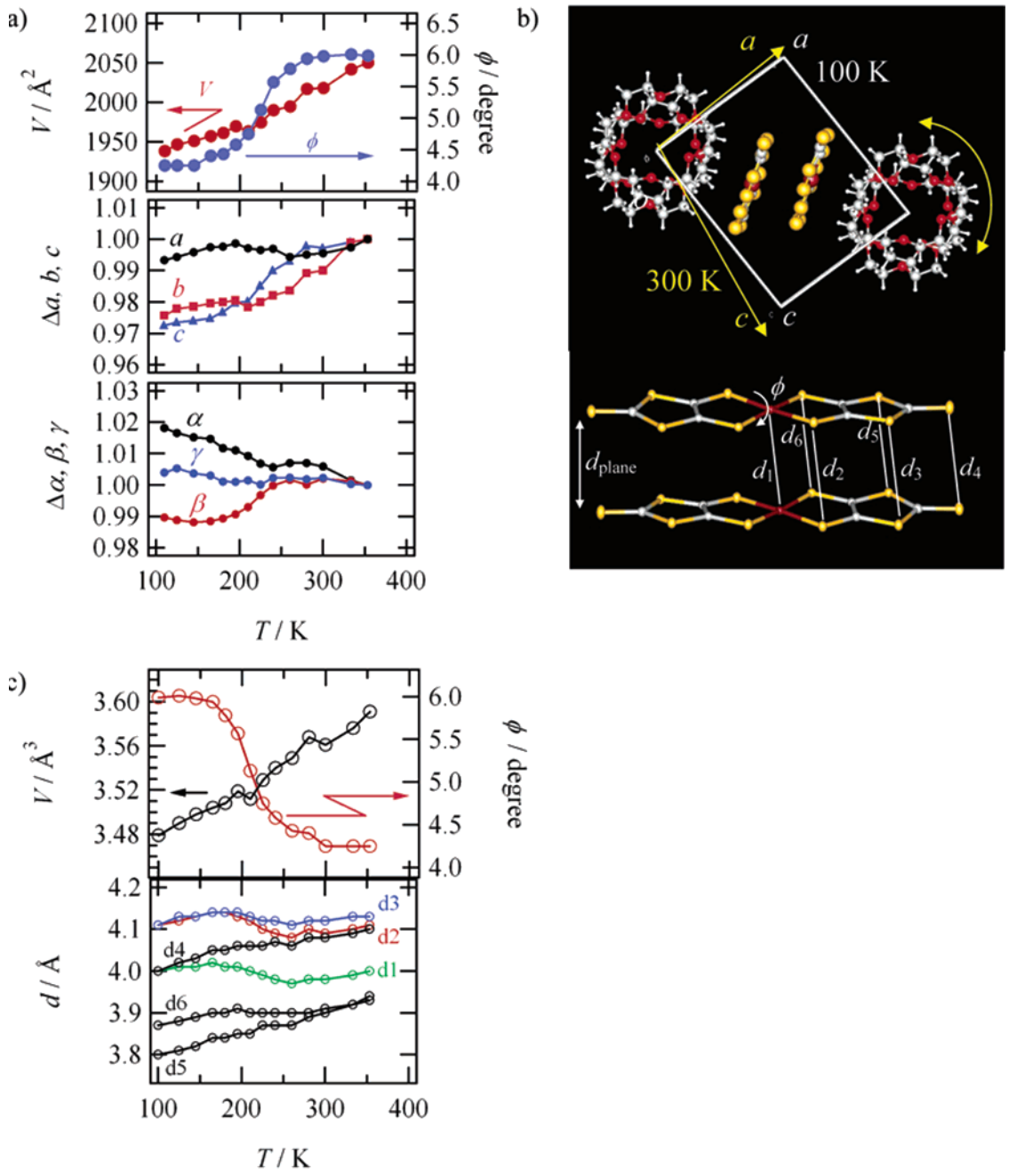

Figure 5. Temperature-dependent crystal parameters. (a) Temperature-dependent crystal volume (V), lattice constant, and dihedral angle between two C_3S_5 planes (ϕ). (b) Schematic lattice modulation from 100 to 300 K (upper figure) and $[Ni(dmit)_2]^-$ π-dimer configuration (lower figure). Temperature-dependent intradimer structural parameters (d_{plane}, ϕ, and d_1-d_6). d_{plane} and angle ϕ are the interplanar distance between two $[Ni(dmit)_2]^-$ mean planes and the dihedral angle between two C_3S_5 planes within the $[Ni(dmit)_2]^-$ molecule, respectively. The d_1-d_6 are intermolecular Ni−Ni and S−S distances within the $[Ni(dmit)_2]^-$ dimer. (c) Temperature-dependent intradimer structural parameters (d_{plane}, ϕ, and d_1-d_6). d_{plane} and angle ϕ are the interplanar distance between two $[Ni(dmit)_2]^-$ mean planes and the dihedral angle between two C_3S_5 planes within the $[Ni(dmit)_2]^-$ molecule, respectively. The d_1-d_6 are intermolecular Ni−Ni and S−S distances within the $[Ni(dmit)_2]^-$ dimer.

showing that C_{ex} originates from the independent orientations of three [18]crown-6 molecules of the $Cs_2([18]crown\text{-}6)_3$ cation, each having two positions (as observed in the X-ray analysis). Because the temperature-dependent C_{ex} exhibited a broad maximum, the stopping of the molecular rotation is not a first-order phase transition. The rotations of [18]crown-6 are not independent within the crystal, but are somewhat synergetic; the rotations, however, are not correlated over the entire crystal.

Above 200 K, [18]crown-6 exhibited thermally activated molecular motion, which largely influences the magnetic properties of the crystal. The temperature-dependent molar magnetic susceptibility per one $[Ni(dmit)_2]^-$ molecule (χ_{mol}) is shown in Figure 4. The magnetic exchange energy (J) within the π-dimer is also indicated. The magnetic exchange energy is proportional to the square of the transfer integral, $|J| = 4t^2/U_{eff}$, where U_{eff} is the effective on-site Coulomb repulsive energy in the solid.[21] The intradimer interaction ($t_1 = 110$ meV at 100 K) based on the extended Hückel molecular orbital calculation was significantly stronger than other interdimer interactions (~0.1 meV). The π-dimer is magnetically isolated within the crystal. Accordingly, the magnetic property is dominated by that of the $[Ni(dmit)_2]^-$ π-dimer with the singlet spin ground state.

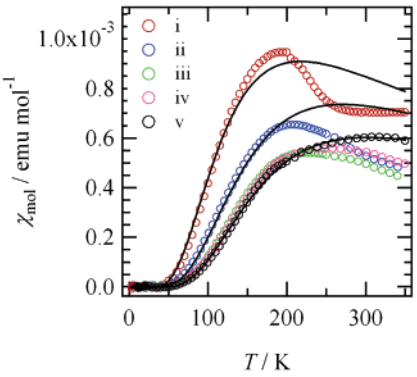

Figure 6. Temperature- and pressure-dependent magnetic susceptibility of $Cs_2([18]crown\text{-}6)_3[Ni(dmit)_2]_2$. χ_{mol} at (i) 0, (ii) 0.6, (iii) 1.1, (iv) 2 kbar, and (v) 4 kbar. The solid lines correspond to curve fitting of the S−T model, in which C and J are a constant and a fitting parameter, respectively.

Over the temperature range from 4 to 160 K, the $\chi_{mol}-T$ behavior of salt **1** was fitted using the singlet−triplet (S−T) thermal excitation model with a fixed Curie constant of 0.396 emu·K mol^{-1}, obtained using EPR measurements ($g = 2.051$, $\Delta H = 102.3$ mT), and variable $J = -218$ K. As expected from the dimeric structure of $[Ni(dmit)_2]^-$, the $\chi_{mol}-T$ behavior at lower temperatures showed good agreement with the S−T model. Above 160 K, however, significant deviations from the S−T model were observed, with a broad maximum of χ_{mol} at ∼200 K.

The temperature corresponding to the maximum χ_{mol} was comparable to that at which the [18]crown-6 molecules start to rotate. Typically, J values are nearly temperature-independent due to the consumption of the uniform thermal contraction of a crystal lattice between t and U_{eff}, both of which increase with decreasing temperature. However, as shown in Figure 4, a minimum was observed for J at ∼180 K ($t_1 = 90$ meV). The temperature-dependent J values were incorporated into the S−T model. The results of the fit were almost identical to that of the $\chi_{mol}-T$ behavior above 160 K (brown line), indicating that deviations from the simple S−T model are attributable to the changes in intradimer interactions between the $[Ni(dmit)_2]^-$ anions. On the basis of the temperature dependences of the intradimer transfer integrals, ^{1}H NMR spectra, ^{133}Cs NMR spectra, specific heat, and magnetic susceptibility, it can be concluded that molecular rotation and magnetic properties are strongly coupled within the crystal.

Because the $[Ni(dmit)_2]^-$ π-dimer was sandwiched between layers of molecular rotors (Figure 1a), the $[Ni(dmit)_2]^-$ configuration within the dimer is affected by molecular rotation. The mechanism of coupling between magnetic exchange interactions and molecular rotation was examined in detail using the temperature-dependent crystal structure (Figure 5). Although a linear increase of the unit cell volume (V) from 1832.9(2) ($T = 100$ K) to 1938.8(2) Å^3 ($T = 352$ K) was confirmed, deviations from linearity were observed in the c-axis and β-angle at ∼220 K, which is consistent with the temperature at which [18]crown-6 starts to rotate. Moreover, the dihedral angle between two C_3S_5 planes (ϕ) exhibited an abrupt change at ∼220 K. Lattice modulation induced by the rotation of [18]crown-6 affected the $[Ni(dmit)_2]^-$ conformation (from planar to slightly twisted) and increased the t_1 interaction and intradimer magnetic exchange energy.

Because molecular rotation has been confirmed within the crystal, the next step is to realize unidirectional rotation in the solid state. At least two conditions are essential for the unidirectional rotation: introduction of an asymmetric potential for rotation, and perturbation of the potential energy. Mechanical braking of the rotation by applying hydrostatic pressure is an example of an external stimulus for such a perturbation. We examined the temperature dependence of $\chi_{mol}-T$ behaviors under hydrostatic pressure (Figure 6). By applying pressure, deviation from the S−T model was gradually suppressed, and the $\chi_{mol}-T$ behavior was almost identical with that of the S−T model at 4 kbar. At this pressure, molecular rotation can be stopped over the entire range of measured temperatures—in other words, the molecular rotation in the crystal can be externally biased by applying pressure. Although the pressure required to stop molecular rotation completely at room temperature is relatively high, perturbation of the potential can be achieved at much lower pressures.

Summary

A supramolecular rotor structure of $Cs_2([18]crown\text{-}6)_3$ was introduced as a countercation into a magnetic $[Ni(dmit)_2]^-$ single crystal, in which molecular rotation and magnetic behavior are strongly coupled. Temperature-dependent X-ray structural analyses, ^{1}H and ^{133}Cs NMR, and specific heat studies confirmed the rotation of [18]crown-6 above 220 K. The $[Ni(dmit)_2]^-$ anions formed strong π-dimers, possessing a magnetic ground state with a singlet spin. At higher temperatures, significant deviations from the S−T model were observed, which can be explained as changes in the intradimer transfer integrals (t_1). Rotation of [18]crown-6 caused changes in the strength of the intradimer magnetic interactions through intermolecular forces between the supramolecular cation and the $[Ni(dmit)_2]^-$ anion. The molecular rotation was controlled externally by the application of pressure. The unidirectional molecular rotation in the solid state, coupled with the electronic system, has a potential to convert kinetic energy to electromagnetic energy with high efficiency.

Acknowledgment. This work was partly supported by a Grant-in-Aid for Science Research from the Ministries of Education, Culture, Sports, Science, and Technology of Japan. The authors thank Dr. K. Ichimura and Prof. K. Nomura for allowing the use of their SQUID magnetometer.

Supporting Information Available: Temperature-dependent crystal data of **1**, electrical conductivity, and ESR spectrum at 298 K (PDF, CIF). This material is available free of charge via the Internet at http://pubs.acs.org.

JA043527A

(21) (a) Scott, J. C. In *Semiconductor and Semimetals. High Conducting Quasi-One-Dimensional Organic Crystals*; Conwell, E., Ed.; Academic Press: New York, 1988; p 385. (b) Carlin, R. L. *Magnetochemistry*; Springer-Verlag: Heidelberg, 1986. (c) Kahn, O. *Molecular Magnetism*; Wiley-VCH: New York, 1993.